

A low-weight Plasma Instrument to be used in the Inner Heliosphere

T. H. Zurbuchen^a, G. Gloeckler^{a,b}, J. C. Cain^b, S. E. Lasley^b, and W. Shanks^b

^a Space Physics Research Laboratory, The University of Michigan,
2455 Hayward Street, Ann Arbor, MI 48109-2143, USA

^b Department of Physics and IPST, University of Maryland, College Park, MD 20742, USA

ABSTRACT

In the proposed Mercury-Messenger mission, a satellite will approach the Sun to a distance of around 0.3 AU. A plasma instrument to be flown on this satellite provides a unique possibility to probe the inner heliosphere in a distance range which has previously only been investigated by the Helios missions. In addition, *in situ* observations of the low-energy ions in the Mercury magnetosphere can be performed for the first time. In some phases of the orbit pick-up ions from Mercury are also expected to be detected.

Because of the tight mass constraints on this mission, a new low-weight plasma instrument FIPS (Fast Imaging Particle Spectrometer) was developed which is particularly suited for this near-solar plasma environment. It is a combination of an electrostatic deflection system and a linear time-of-flight system. Using numerical simulations we demonstrate the properties of this design and discuss possible applications.

Keywords: Solar wind plasma, solar instrumentation, mass spectrometer, plasma composition, mass spectrometry, Planet Mercury

1. INTRODUCTION

The increasing interest in Mercury has to do with the fact that it is the only mostly unexplored terrestrial planet. Its close vicinity to the Sun and the interior magnetic field of Mercury provides a very interesting test-case for the interaction of solar wind with terrestrial planets. Ultimately, the measurements on Mercury will thus help to understand the solar-terrestrial interactions. In addition, pick-up ions from Mercury provide a very important, well defined test-case for mass-loading in the solar system.

The Mercury-Messenger mission is also of interest because it gives the opportunity of *in situ* analysis of the solar wind using modern plasma instrumentation. In this paper we will concentrate on this particular aspect. In the late 70s and early 80s the Helios spacecraft did the first - and until now the only - measurements of the solar wind close to the Sun.¹ It is now evident that the structure of the solar wind is very different for heliospheric distances closer to 1 AU than what is known for distances ≥ 1 AU. At heliospheric distances around 1 AU, the solar wind shows signatures of plasma interactions occurring in the heliosphere which increasingly mask the solar-induced properties.² At 0.3 AU, these effects are much weaker and therefore, solar plasma patterns much clearer. There are two different developments which make an inner heliosphere mission very interesting at this time. First of all, there are new solar observations, and secondly, inner sources of particles, probably related to dust, have recently been discovered. We will discuss these observations very briefly and then put them into the context of an inner-heliosphere mission.

During the last years a large amount of data coming from various experimental programs such as the Solar and Heliospheric Observatory (SOHO)³ have provided new insight into the physics of the Sun, particularly its outer atmosphere. Using the Large-Angle and Spectrometric Coronagraph (LASCO) and the Ultraviolet Coronagraph Spectrometer (UVCS) it has been made possible, to remotely investigate the solar plasma close to the Sun as it escapes to form the solar wind.⁴ The results from these instruments indicate that the solar wind close to the Sun is strongly affected by small-scale wave-particle interactions. Oxygen kinetic temperatures show values which can be up to an order of magnitude larger than the H kinetic temperature at the same heliocentric distance. This has been interpreted to be a reliable tracer of the solar wind acceleration process. However, the interpretation of these remote-sensing results are not straight-forward. A spacecraft at 0.3 AU should be able to observe these non-thermal

Send correspondence to T.H.Z. E-mail: thomasz@umich.edu

distributions and provide a very solid test for new solar wind theories which have been triggered by these UVCS results.

Using Ulysses-SWICS data, a new extended inner source of pick-up ions has recently been discovered.⁵ Neutral gas in the inner heliosphere is being ionized and subsequently picked up by the solar wind. This material is presumably associated with interstellar and interplanetary dust⁶ and therefore carries crucial information about the history of the solar system. It is difficult to identify the details of the source regions from measurements around 1 AU. An inner-heliosphere plasma experiment could provide the key-observation for the correct interpretation of this result. In order for this to happen, it is very important to accurately determine the distribution functions of these singly charged particles as a function of heliocentric radius.

All of the above mentioned observations indicate in one sense or another that the internal state of the solar wind plasma, the distribution functions of its components, and its composition are of major importance for the understanding of the physical processes in the inner heliosphere.

In this paper, we describe a plasma analyzer optimized for such *in situ* measurements in the inner heliosphere. First, we will infer instrument requirements based on previous observations and theories. Section 3 will then describe the new sensor and finally, Section 4 summarizes numerical simulations.

2. REQUIREMENTS FOR FIPS

2.1. Requirements due to Plasma Properties

Traditional plasma instruments probing the solar wind at heliospheric distances around 1 AU often consist of an electrostatic deflection system and a channeltron detector.⁷ At around 1 AU heliospheric distance these analyzers can separate the distribution functions of H^+ and He^{2+} under most circumstances. After integrating over the solid angle, it is also possible to separate O, Si, and Fe contributions when the kinetic temperature is unusually low. Various other techniques have successfully been applied which manage to identify solar wind components based on their mass per charge M/Q (e.g., the Ion Composition Experiment on ISEE3⁸) or even based on measurements of M and Q separately (e.g., the Solar Wind Ion Composition Spectrometer on ACE⁹ or, SWICS on Ulysses¹⁰).

For solar wind protons the kinetic temperature at 0.3 AU heliospheric distance was previously observed to be up to $\sim 7 \cdot 10^5$ K.¹ Under these circumstances it is nearly impossible to effectively separate the solar wind components based on their energy per charge ratio E/Q . Independent M/Q detection is required in addition to E/Q analysis in order to be able to analyze the relatively rare and hot ions at 0.3 AU and also ions, particularly from Mercury.

It is also important to have the full, three-dimensional velocity distributions available in order to distinguish different sources, i. e., pick-up ions from extended inner sources or from Mercury. The E/Q range of the particles is between ~ 10 V and ~ 10 kV. This range contains low energy Mercury ions, low energy pick-up ions, the solar wind including its minor components and also most of the hot pick-up ions up to mass 16 (Oxygen).

2.2. Technical Requirements

There are additional constraints on the plasma instrument which come from more technical aspects of the Messenger-Mercury mission. The first aspect is directly related to the close vicinity to the Sun: It is very important to be able to suppress potential background signals from energetic particles and high-energy radiation. This implies that in addition to very good mechanical shielding, a coincidence technique should be used for the measurements. This prevents noise in the electronic system from dramatically reducing the sensitivity and also the dynamic range of the sensor.

The mass of the instrument is also highly constrained. Because of the large delta- v required to inject a satellite into a Mercury orbit, the spacecraft mass, and therefore also the mass of the instruments, has to be kept as low as possible.

Messenger will be a three-axis stabilized spacecraft. Therefore, the plasma analyzer is required to have a large field-of-view.

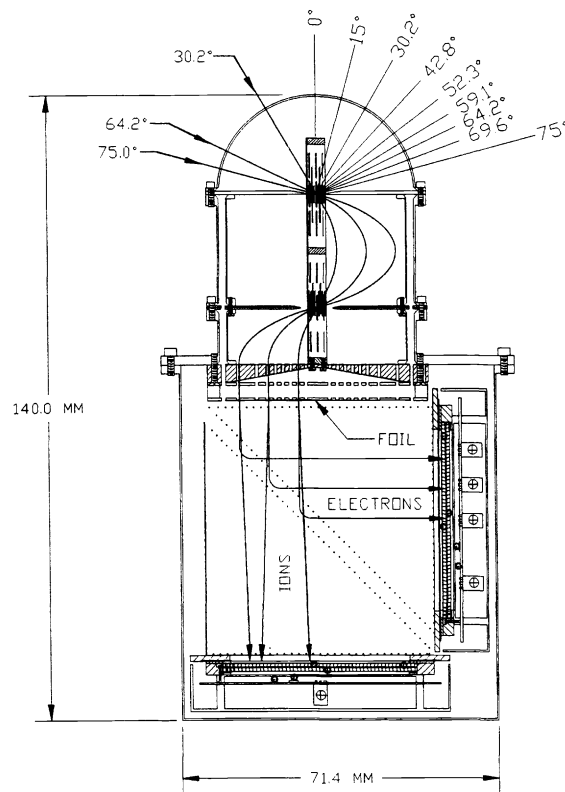


Figure 1. Cross-section through the analyzer with ion-trajectories. For detailed descriptions refer to text.

3. THE FAST IMAGING PLASMA SPECTROMETER (FIPS)

3.1. Overview

Based on the above-mentioned design criteria, a plasma instrument design has been developed. The system was introduced as part of a comprehensive package to do *in situ* and remote sensing observations near the Sun (McNutt et al. (1996)¹¹) and has been adapted here to meet the design criteria mentioned above. Figure 1 shows the basic principle of the analyzer: Ions enter the sensor through one of the over 100 1 mm² holes and are deflected in a cylindrical deflection system with variable voltage U . After a post-acceleration with U_{post} , they are detected in a time-of-flight system with position sensing. This design unambiguously determines the incoming ion velocity \mathbf{V} and M/Q for all detected ions. For an analyzer voltage (U) range from 10 V to ~ 10 kV, the system covers the required energy range described in section 2. During a voltage cycle period of < 1 min, distribution functions of H, He, O, Fe and all other separable plasma components are determined. The detector has a sufficiently large geometrical field-of-view required for this mission.

In the next section, the analysis procedure is first explained in more detail. We then discuss the mechanical properties of this setup.

3.2. Principle of Operation

The basic elements of particle identification are based on a combination of a collimator, a deflection system, post-acceleration and a linear time-of flight section with position sensing. Figure 2 schematically shows the principle of operation of the analyzer and illustrates the function of the four sub-systems used:

1. Particles with velocity \mathbf{V} , mass M and charge Q enter the sensor through a system of over 100 ~ 1 mm² openings in a spherical dome. These holes allow ions from a solid angle of $\sim 2\pi$ sr access to FIPS.

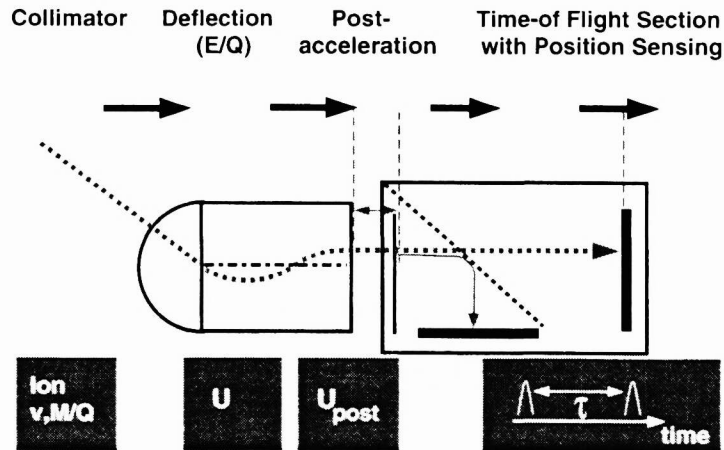


Figure 2. Schematic of the measurement technique used in the new sensor, showing the functions of the four basic elements.

2. The deflection system serves as a UV trap and energy per charge (E/Q) filter, allowing only ions within a given energy per charge range (determined by the stepped voltage and the actual hole location through which the particles enter) access to the time-of-flight system. This E/Q filtering is attained by a system of slits in the deflection system. These slits also filter out scattered particles and photons in the deflection system and prohibit their access into the time-of-flight section. One voltage scan is performed within less than one minute.
3. The particles are post-accelerated in a ≤ 5 kV potential just before entering the time-of-flight section. This energy gain increases the detection probability of the particles and improves the accuracy of the time-of-flight measurement.
4. In the time-of-flight (TOF) section the speed of each ion is determined Position sensing is used to establish the incoming velocity direction of each ion.

The simultaneous measurements of the time-of-flight τ and the position information for a given voltage setting U and U_{post} unambiguously determines \mathbf{V} and M/Q of the detected particle as follows:

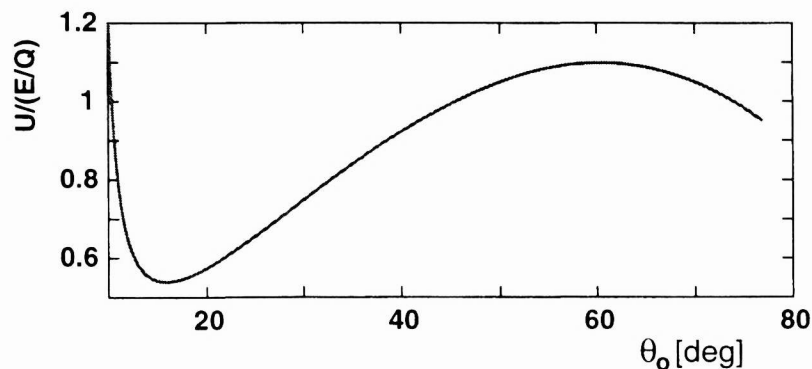


Figure 3. Analyzer constant as a function of incidence angle θ_0 . For a given analyzer voltage U , the E/Q of the analyzed particles depends on the entrance location on the collimator.

First, we define the analyzer constant of the deflection system as a geometry dependent function as given by equation 1.

$$\eta(\theta_0) = \frac{MV_{\theta_0}^2}{2QU} \quad (1)$$

Here, V_{θ_0} is the speed of ideally transmitted particles entering the analyzer from a certain direction. $\eta(\theta_0)$ is analyzer specific and fully determined by the actual geometry of the electrodes. It is shown in Fig. 3 as a function of θ_0 , the co-latitude of the deflection system ($\theta_0 = 0$, if \mathbf{V} is parallel the symmetry axis of the analyzer).

The figure shows, that for a given analyzer voltage U , the energy per charge of transmitted particles is typically larger for particles with smaller angles to the symmetry axis. The energy range of analyzed particles at one particular voltage setting varies within a factor of ~ 2 .

It is then,

$$M/Q = \frac{2(U\eta(\theta_0) + U_{post})\beta \cdot \tau^2}{d^2}, \quad (2)$$

where $\eta(\theta_0)$ is defined by Equation 1, U and U_{post} are the analyzer and post-acceleration voltage, d stands for the distance between *start* and *stop* anode, and β takes into account the energy loss of a particle when penetrating the Carbon foil.

In Equation 2 the M/Q measurement is dependent on the particle velocity \mathbf{V} through $\eta(\theta_0)$. However, the position information \mathbf{p} unambiguously determines the location (θ_0, ϕ_0) where the particle entered. The factor $\eta(\theta_0)$ is then a known quantity and Equation 2 unambiguously determines M/Q . Similarly, the angular information together with Equation 1 determines the initial particle velocity vector \mathbf{V} .

3.3. Technical Aspects

The new design combines previously flown and therefore well understood technology: The deflection system is a cylindrical analyzer used in the direction of its symmetry axis. The linear time-of-flight section combined with a post-acceleration is now a very well known component of many space plasma instruments^{9,10} The position sensing has been previously used, too.¹²

The mass of the entire deflection system is only somewhat more than 1 lbs and the total power consumption is expected to be < 1 W. Table 1 shows a break-down of mass and power into the various sub-systems.

Table 1. Mass and Power requirements of the plasma analyzer.

Subsystem	Mass [g]	Power [mW]
Deflection system	100	
- Power Supply	80	350
2 MCPs	160	
- Position Sensing System	75	
- MCP Enclosure	30	
- Power Supply	120	350
Total	565	700

The background rejection properties of the new system are excellent. First, the constraining slit-system in the deflection analyzer effectively prevents background particles and electro-magnetic radiation from entering the time-of-flight section. Additional background suppression is obtained by using a coincidence technique in the time-of-flight section. The position determination helps to eliminate additional background when processing the data.

4. FIPS SIMULATIONS

This section will concentrate on the electrostatic deflection system. This part of the instrument has not been flown before and is therefore the least understood sub-system. This chapter will first introduce the ion-optical simulation technique and then summarize the basic results relevant to the observations during a Mercury mission.

4.1. Numerical Simulation Technique

The electrostatic deflection system consists of two concentric cylindrical anodes. The potential, Φ , on the outer anode is given by a variable voltage U between 10 V and 10 kV for ions. The inner smaller-radius anode is always at $\Phi = 0$. Ideally, the potential between the two the anodes is therefore given by

$$\Phi(r) = U \frac{\ln(r/r_{in})}{\ln(r_{out}/r_{in})}. \quad (3)$$

Here, r_{out} is the radius of the outer, r_{in} , the radius of the inner electrode. U is the voltage applied to the outer electrode.

Field control rings cause deviations from this ideal configuration to be small and also fringe fields are expected to only be of minor importance for ion-trajectories. With these approximations, the Lagrange-function of the particle motion in cylindrical coordinates (r, ϕ, z) is given as:

$$\mathcal{L} = \frac{1}{2}M\left[\left(\frac{d}{dt}r\right)^2 + r^2\left(\frac{d}{dt}\phi\right)^2 + \left(\frac{d}{dt}z\right)^2\right] - QU \frac{\ln(r/r_{in})}{\ln(r_{out}/r_{in})} \quad (4)$$

For \mathcal{L} the equations of motion can be calculated using the Euler-Lagrange equations.

$$M \frac{d^2}{dt^2}r = mr\left(\frac{d}{dt}\phi\right)^2 - \frac{QU}{\ln(r_{out}/r_{in}) \cdot r} \quad (5)$$

$$\frac{d}{dt}\left[Mr^2\left(\frac{d}{dt}\phi\right)\right] = 0 \quad (6)$$

$$\frac{d^2}{dt^2}z = 0 \quad (7)$$

Equation 6 describes the conservation of the angular momentum for rotations perpendicular to the symmetry axis of the system. For our configuration, ideally $\frac{d}{dt}\phi = 0$ at all times, and Equ. 5 simplifies accordingly. For all other motions, $rv_\phi = \text{constant}$, resulting in a faster rotation close to the inner electrode. For ideal trajectories Equation 5 can be integrated to give an upper limit for the velocity in r -direction $v_r = \left(\frac{2QU}{M \ln(r_{out}/r_{in})}\right)^{1/2}$. It turns out to be rather difficult to calculate the analytical solutions for $r(t)$. Solutions can only be written as integrals of Error-functions. Particle trajectories are most easily calculated by numerical integration of Equ. 5-7. We use a standard adaptive step-size Runge-Kutta algorithm, which conserves the energy of the particles up to $\sim 10^{-6}$ with a very reasonable calculation effort. We then use Monte-Carlo techniques to determine the instrument respond to realistic particle distribution functions.

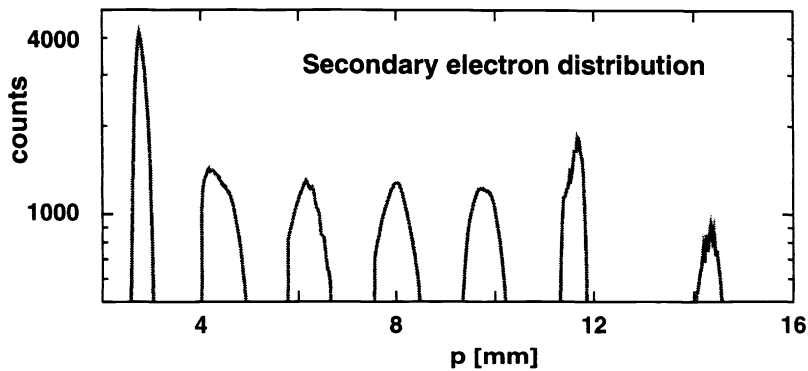


Figure 4. Spatial distribution of secondary electrons from the Carbon foil caused by particles entering through a set of openings. The calculations show, that the incident direction is clearly resolved.

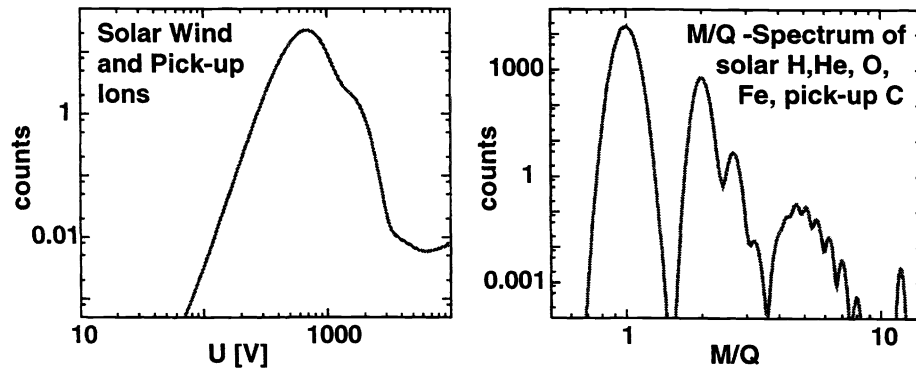


Figure 5. Solar wind simulation. Left: Voltage scan of the start rate from ions entering the 30.2 deg hole. Notice, that it is impossible to separate various ion species with the electrostatic deflection system. Right: Data after analyzing it with the time-of-flight system. Here, the data has been integrated over all energies. particles are

4.2. Results of Numerical Calculations

First, we use the numerical simulation technique to calculate the E/Q of ideally transmitted particles for a given voltage and plot them in Fig. 3 as a function of θ_0 . The solution depends on the actual geometry of the deflection analyzer. Here we assumed a geometry in accordance with Fig. 1: electrode radii $r_{in} = 2$ mm, $r_{out} = 20$ mm, analyzer height $h = 40$ mm. For one particular voltage setting particles of various E/Q (dependent on θ_0) penetrate the deflection system.

We mentioned previously that the analyzer system relies on the fact that particles entering through different holes can be effectively separated. This is tested by simulating a isotropic distribution function entering through the set of holes shown in Fig. 1. Figure 4 shows the result of this simulation. A one-dimensional cut through the spatial distribution of secondary electrons from the Carbon foil is shown. Particles, entering through the various holes are clearly resolved. Holes at increasing θ_0 angles are mapped to increasing p -values. This result also demonstrates that neighboring holes do not have significant cross-talk.

Finally, we calculate a simulation of solar wind and pick-up ions at 0.3 AU. The solar wind is assumed to have a speed of 400 km/s and a mass-proportional temperature of $5 \cdot 10^5$ K/amu. The C pick-up ions are assumed to have a shell-distribution. The left-hand side of Figure 5 shows the start-rate of secondary electrons for a solar wind ion distribution including H, He, O and Fe as well as inter source C pick-up ions entering through the (arbitrary) hole at $\theta_0 = 30.2$ deg. It is evident, that the various particle components can not be separated and the mass per charge analysis is necessary to calculate actual estimates for the distribution functions. The right-hand side of Fig. 5 shows solar wind now analyzed with the time-of-flight spectrometer integrated over the entire voltage cycle. H, He, are clearly resolved, and also, the various O and Fe charge states are separated. The resolving power of the instrument makes it possible to calculate actual freeze-in temperatures similar to SWICS-ACE.⁹ Notice the peak at $M/Q = 12$, where the inner source C ions are well visible in this simulation. Table 2 summarizes analyzer properties as a result of the simulations.

Table 2. Properties of the new analyzer.

Energy range	10 eV/charge - ~ 12 keV/charge
Angular range	$\sim 2\pi$ sr
Energy acceptance (per hole, $U = const.$)	5 %
Angular acceptance (per hole)	5 deg
Mass/Charge resolution	> 10
Time for one complete spectrum	< 1 min (adjustable)

5. SUMMARY

We introduced requirements for a plasma detector to be flown on a Mercury Messenger mission to 0.3 AU and then described the Fast Imaging Plasma Analyzer (FIPS) which is found to be consistent with the observational and technical constraints of such a mission. It is a low-weight, low-power detector combining a cylindrical electrostatic deflection system and a linear time-of-flight system with position sensing. The new deflection geometry has successfully been tested and optimized with an extensive simulation effort. For the time-of-flight system we use well-tested and previously flown technology. We find that FIPS manages to measure full 3-D distribution functions of the major constituents of the solar wind and also can resolve inner source pick-up ions. The analyzer is of very low mass and reasonable power consumption.

Finally, notice that FIPS is very versatile and can be adapted for different purposes. If, for example, a negative analyzer voltage is applied, electron distribution functions can be determined with the same deflection system. FIPS could therefore be used as part of an instrument package for a mission close to the Sun.¹¹

ACKNOWLEDGMENTS

We thank L. A. Fisk and P. Bedini for many useful discussions. This work has been supported, in part, by the Space Research Laboratory of the University of Michigan.

REFERENCES

1. Schwenn, R., "Large-scale structure of the interplanetary medium", in *Physics of the Inner Heliosphere I.*, R. Schwenn, E. Marsch, ed., Springer 1990.
2. Marsch, E., "Kinetic physics of the solar wind plasma", in *Physics of the Inner Heliosphere II.*, R. Schwenn, E. Marsch, ed., Springer, 1990.
3. Domingo, V., B. Fleck, and A. I. Poland, "SOHO: The Solar and Heliospheric Observatory", *Space Sci. Rev.*, **72**, 81, 1995.
4. Kohl, J. L. *et al.*, "First results from the solar ultraviolet coronagraph spectrometer", *Solar Phys.*, **175**, 613, 1997.
5. Geiss, J., G. Gloeckler, and R. von Steiger, "Origin of C⁺ ions in the heliosphere", *Space Sci. Rev.*, **78**, 43, 1996.
6. Gloeckler, G., and J. Geiss, "Interstellar and inner source pickup ions observed with SWICS on Ulysses", *Space Sci. Rev.*, in press, 1998.
7. McComas, D. J., S. J. Bame, P. Barker, W. C. Feldman, J. L. Phillips, P. Riley, J. W. Griffee, "Solar wind electron proton alpha monitor (SWEPAM) for the Advanced Composition Explorer", *Space Sci. Rev.*, in press, 1998.
8. Coplan, M. A., K. W. Ogilvie, P. Bochsler and J. Geiss, "Ion composition experiment", *IEEE Trans. on Geosci. Electr.*, **GE-16**, 185, 1978.
9. Gloeckler, G., J. Cain, F. M. Ipavich, E. O. Tums, P. Bedini, L. A. Fisk, T. H. Zurbuchen, P. Bochsler, J. Fischer, R. F. Wimmer-Schweingruber, J. Geiss, and R. Kallenbach "Investigation of the composition of solar and interstellar matter using solar wind and pickup ion measurements with SWICS and SWIMS on the ACE spacecraft", *Space Sci. Rev.*, in press, 1998.
10. Gloeckler, G., J. Geiss, H. Balsiger, P. Bedini, J. C. Cain, J. Fischer, L. A. Fisk, A. B. Galvin, F. Gliem, D. C. Hamilton, J. V. Hollweg, F. M. Ipavich, R. Joos, S. Livi, R. Lundgren, U. Mall, J. F. McKenzie, K. W. Ogilvie, F. Ottens, W. Rieck, E. O. Tums, R. von Steiger, W. Weiss, and B. Wilken, "The solar wind ion composition spectrometer", *Astron. Astrophys. Suppl. Ser.*, **92**, 267, 1992.
11. McNutt R. L., R. B. Gold, E. P. Keath, D. M. Rust, S. M. Krimigis, L. J. Zanetti, C. E. Willey, B. D. Williams, W. S. Kurth, D. A. Gurnett, M. H. Acuna, L. Burlaga, G. Gloeckler, F. M. Ipavich, A. J. Lazarus, J. T. Steinburg, G. E. Brueckner, D. G. Socker, T. E. Holzer, P. Bochsler, R. Kallenbach, and A. Roux, "Advanced Solar Probe Experiment Module (SOLEM)", *Proc. SPIE*, **2804**, 2, 1996.
12. Hovestadt, D. *et al.*, "CELIAS - Charge, Element and Isotope Analysis System for SOHO", *Solar Phys.*, **162**, 441, 1995.